Identification of Amino Acids Important for the Biochemical Activity of *Methanothermobacter thermautotrophicus* MCM

Ryan J. Fletcher,[‡,§] Jingping Shen,[‡,||] Lauren G. Holden,[§] and Xiaojiang S. Chen*[,§]

Molecular and Computational Biology, University of Southern California, Los Angeles, California 90089-2910, and Biochemistry and Molecular Genetics, University of Colorado Health Sciences Center, Denver, Colorado 80262

Received January 7, 2008; Revised Manuscript Received May 16, 2008

ABSTRACT: *Methanothermobacter thermautotrophicus* minichromosomal maintenance protein (mtMCM) is a 75 kDa protein that self-assembles into a double hexamer structure. The double hexamer formed by the N-terminal region of mtMCM has a highly charged (overwhelmingly net positive) inner channel. Here we investigate the effects of point mutations of some of these charged residues on the biological activities of mtMCM. Although all of the mutants were similar to the wild type in protein folding and complex assembly, we found that mutations impaired helicase activity. The study of the DNA binding and ATPase activities of these mutants revealed that the impairment of the helicase activity was highly correlated with a decrease in DNA binding, providing evidence consistent with the role of these charged residues of the inner channel in interactions with DNA.

The progression from G_1 to S phase during the cell cycle is highly regulated. A group of proteins essential for the successful transition and the completion of S phase are the minichromosomal maintenance proteins (MCM). The MCM proteins in eukaryotes are a subgroup of six proteins (MCM2−7) within the much larger AAA+ ATPase family (*1*). MCM2−7 share a highly similar stretch of amino acids referred to as the MCM box (*2–4*) located in the C-terminal half of the protein. The MCM box contains the Walker A and Walker B motifs responsible for the binding and hydrolysis of ATP.

MCM proteins play an important role in the initiation of replication, as these proteins serve as replication helicases for fork unwinding. During G_1 phase, origins with the potential to serve as sites for the initiation of DNA replication are marked by an origin recognition complex (ORC). Subsequent binding by Cdc6 and Cdt1 promotes the recruitment of MCM proteins to form the prereplication complex (pre-RC). Failure to recruit MCM proteins results in loss of origin firing and G1-phase arrest. Ensuing activity by both Dbf4 dependent kinase (DDK) and cyclin dependent kinase (CDK) promotes the binding of Cdc45 and recruitment of a number of replication proteins to the pre-RC, ultimately leading to the initiation of replication. The presence of all six MCM proteins is necessary for entry and completion of S-phase (reviewed in refs *5–7*.

Methanothermobacter thermautotrophicus has a single MCM (mtMCM) protein that has the ability to self-assemble into a double hexamer structure (*8–13*). Purified mtMCM protein contains ATPase, DNA binding, and helicase activities *in vitro*. The crystal structure of the N-terminal portion of double-hexameric mtMCM (N-mtMCM) revealed an overwhelmingly net positively charged inner channel surface (*10*). Here we investigated the functional role of five residues located on the inner channel surface of the double hexameric N-mtMCM structure. Mutational and biochemical studies revealed that these residues play important roles in helicase function.

EXPERIMENTAL PROCEDURES

Cloning and Mutagenesis. The gene for *Methanothermobacter thermautotrophicus* MCM was cloned into the pGEX-2T expression vector using the restriction enzymes *Xho*I and *Xba*I for expression as a GST-MCM fusion protein. Purified wild-type mtMCM protein was always severely degraded, resulting in a heterogeneous population. We identified the two major cleavage sites for this degradation by N-terminal sequencing and mass spectrometry of the degraded protein fragments (data not shown). These two cleavage sites occurred at R275 and R338. To decrease the degradation and provide a more homologous protein product, we generated a mutant with the two arginines mutated to alanines. The degradation of the mutant was greatly reduced compared with the unmodified wild type protein (see Supporting Information Figure 1). At the same time, this mutant protein retained helicase, ATPase, and DNA binding activities at levels similar to those of the wt protein. All the channel surface mutants reported in this study were constructed to also contain these two mutations to eliminate differences in degradation between different constructs. In this study, the construct containing the two arginine to alanine mutations is referred to as wild type (wt). Five charged residues on the channel surface, R116, K117, R122, K178, R223 (Figure 1A,B), were all mutated to alanine through standard site-directed mutagenesis methods. The sequences of all clones

* To whom correspondence should be addressed: Molecular and Computational Biology, University of Southern California, Los Angeles, CA 90089-1340. Tel: 213-740-5487. Fax: 213-740-0493. E-mail: Xiaojiang.Chen@usc.edu.

‡ These authors contributed equally to this work.

§ University of Southern California.

|| University of Colorado Health Sciences Center.

10.1021/bi800032t CCC: $40.75
Published on Web 08/29/2008

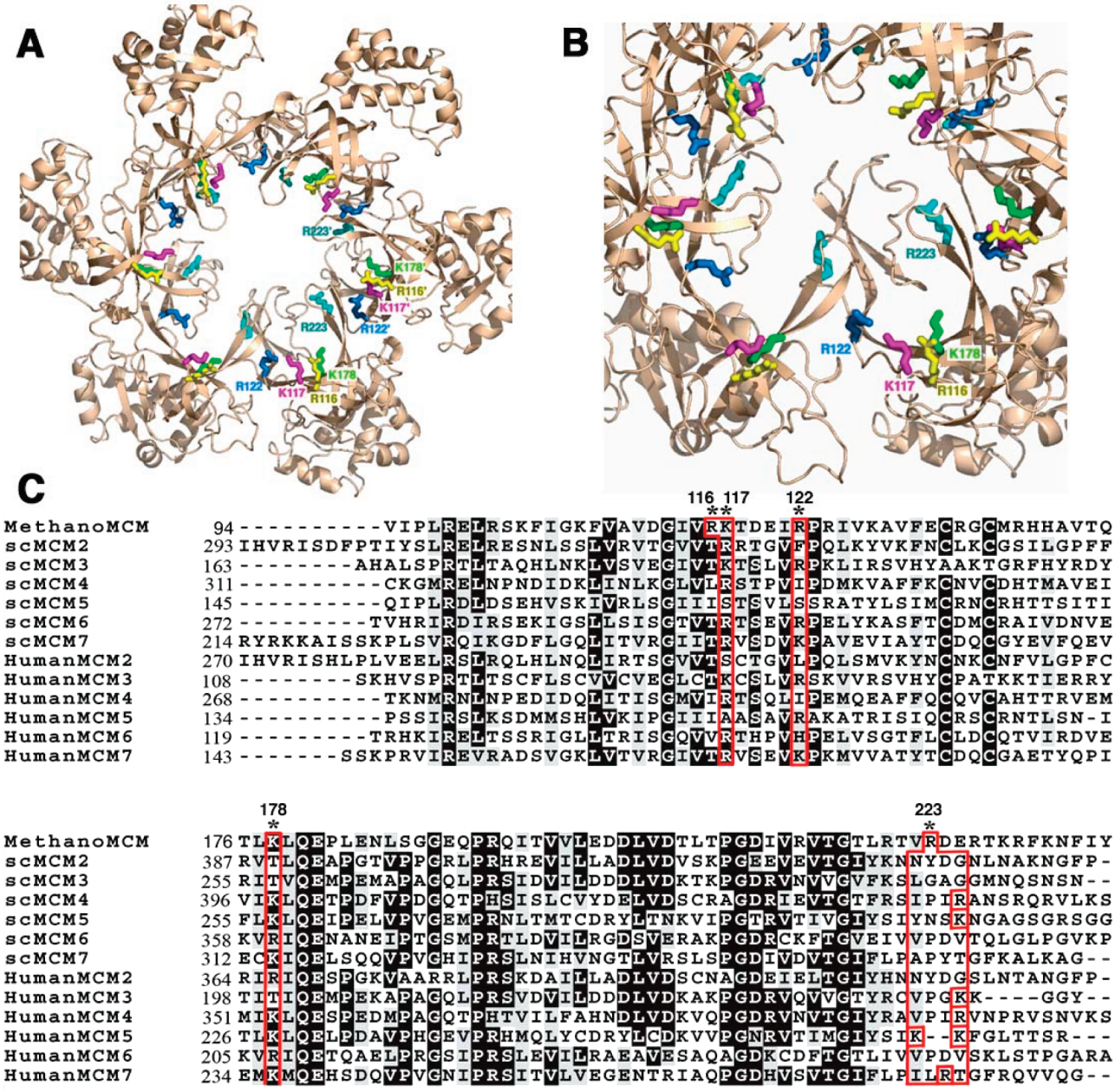

FIGURE 1: Location of the five positively charged residues on the inner channel surface of N-mtMCM. A: N-mtMCM hexamer structure showing the five mutated residues, R116 (yellow), K117 (pink), K178 (green), R122 (blue), and R223 (cyan). B: A closeup of the N-mtMCM view shown in panel A. R223 is on one side of the β-hairpin, R122 is adjacent to the β-hairpin of another monomer. K117 is also on one side of a monomer, around the side channel formed between two neighboring subunits. C: Sequence alignments of mtMCM (methanoMCM) and MCM2−7 from *S. cerevisiae* (scMCM) and humans (humanMCM). Amino acids mutated in this study are marked by asterisks. Red boxes highlight aligned residues that are mutated in this study.

were verified by sequencing the DNA region encoding the entire MCM protein.

Protein Purification. All proteins were grown in *Escherichia coli* cells at 37 °C until $OD_{600} = 0.2$, and then the temperature was reduced to 24 °C. Isopropyl-β-D-thiogalactoside (IPTG) was added to 0.2 mM when $OD_{600} = 0.5$. The cells were shaken at 24 °C overnight. Cell pellets were resuspended in purification buffer (50 mM Tris, pH 8.0, 250 mM NaCl, 10 mM DTT) and sonicated on ice with protease inhibitors pepstatin, leupeptin, and phenylmethylsulfonyl fluoride (PMSF). The GST-MCM fusion protein in the supernatant was separated from other proteins using glutathione resin (Amersham) at 4 °C. After thrombin cleavage of the GST-fusion protein, the free MCM protein was further purified using Superose-6 gel filtration column chromatography (16/60 cm). Peak fractions were collected and purity was analyzed by SDS−PAGE. Protein was concentrated using Amicon Ultra (Millipore) centrifuge devices and quantified using the Bio-Rad protein assay and Coomassie blue staining of an SDS−PAGE gel.

Heat Stability of Mutants. Protein samples (10 μg) were heated at 55 °C in 15 μL of helicase buffer for 30 min. The heat-treated protein was analyzed by Superose-6 column chromatography and on a 10% SDS−PAGE gel.

Helicase Assay. A 60 nucleotide primer $^{5'}$TTT TTT TTT TTT TTT TTT TTT CGC GCG GGG AGA GGC GGT TTG CGT ATT GGG CGC C$^{3'}$ (Operon) was purified and radio-labeled as previously described for DNA binding

assays. The labeled primer was mixed in a 2:1 ratio with M13mp18 circular single-stranded DNA in 300 mM NaCl and 20 mM Tris (pH 8.0), boiled in 900 μL water for 3 min and allowed to cool to room temperature over 5 h. This helicase substrate containing 34 complementary bases and a 26 dT noncomplimentary overhang was purified from excess primer using 700 μL Sephacryl 300HR resin in a 2 mL glass column (Bio-Rad). Fractions containing helicase substrate were pooled and stored at 4 °C. Reactions of 20 μL containing 20 mM Tris (pH 7.8), 10 mM $MgCl_2$, 1 mM DTT, 5 mM ATP, 0.1 mg/mL BSA, helicase substrate, and MCM protein were assembled on ice. The reactions were then incubated at 50 °C for 30 min, 5x stop solution (10 mM EDTA, 0.5% SDS, 0.1% xylene cyanol, 0.1% bromophenol blue, and 50% glycerol) was added and the sample was placed on ice. Reactions were analyzed on a 12% polyacrylamide gel in 1X TBE run on ice for 50 min at 150 V. The gel was dried and then exposed to film and a phosphorimaging plate for quantification.

DNA Binding Assay. All primers (Operon) were resuspended in 10 mM NaOH and purified by FPLC using a Mono-Q 10/100 column (Amersham). Purified DNA was concentrated and quantified using OD_{260}. For the double-stranded DNA (dsDNA) binding assay, complementary primers were mixed, boiled for 10 min in 900 μL of water, and allowed to cool to room temperature overnight. The annealed dsDNA was then purified by FPLC over a Superdex-75 16/60 (Amersham) column in 50 mM NaCl. The DNA used for the single-strand binding was $^{5'}$AAA GCG CTG ACC TAT CGC GTA TAG CTC GAG GA$^{3'}$ and the complementary oligonucleotides used for the double strand binding assay were $^{5'}$GCG CTG ACC TAT CGA CCT ATA CGG TTA GCC$^{3'}$ and $^{5'}$GGC TAA CCG TAT AGG TCG ATA GGT CAG CGC$^{3'}$. The primers were labeled using T4 polynucleotide kinase (NEB) and γ-^{32}P-ATP (Amersham, 3000 Ci/mmol). The labeled primer was purified using Microspin G-25 columns (Amersham) and stored at 4 °C. Reactions of 20 μL were assembled at room temperature with 50 mM NaCl, 5 mM $MgCl_2$, 50 mM Tris (pH 7.8), 1 mM DTT, 0.1 mg/mL BSA, mtMCM protein (between 0.5−1.0 μM), and 15 nM labeled DNA. Reactions were incubated at 25 °C for 30 min and then 5 μL loading buffer (50% glycerol, 0.1% xylene cyanol, and 0.1% bromophenol blue) was added. Reactions were analyzed by gel electrophoresis and by filter binding assay. For gel analysis, the reactions were loaded onto a 2% agarose gel and electrophoresed for 1 h at 80 V in 1X TBE buffer. Gels were dried and exposed to film and phosphorimaging plates for quantification. For filter binding assay, 10 ul reaction mixtures were applied to nitrocellulose filter (Millipore, HA 0.45 mm). The filter was washed with 15 mL of reaction buffer. The radioactivity retained on the filter was quantified by liquid scintillation counting.

ATPase Assay. Reactions (10 μL) containing 50 mM NaCl, 5 mM $MgCl_2$, 50 mM Tris (pH 7.8), 1 mM DTT, 0.1 mg/mL BSA, γ-^{32}P-ATP (Amersham 3000 Ci/mmol), 15 μM cold ATP, and various amounts of MCM proteins were assembled on ice. Reactions were incubated at 50 °C for 30 min, plunged into ice water and 10 mM EDTA was added. Aliquots (5 μL) from each reaction were placed onto a prewashed PEI cellulose TLC plate (EMD Chemicals INC) and run for two hours in 2 M acetic acid and 0.5 M LiCl. Plates were dried and exposed to film and phosphorimaging plates for quantification.

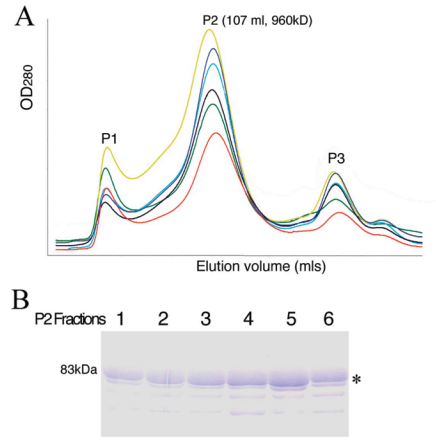

FIGURE 2: Gel filtration analysis of wt and mutant mtMCM proteins. A: FPLC overlay of OD_{280} curves from wt (blue) and the five mutant proteins run on a preparative grade Superose 6 column. The profiles of all proteins overlapped. Peak 1 (P1) is in the void volume, P2 contains protein that has an apparent molecular weight (Mwt) of approximately 960 kDa, and peak 3 (P3) contains degraded protein that cannot oligomerize. P2 has an apparent molecular weight consistent with that of a double hexamer. B: SDS−PAGE analysis of the peak fraction of P2 for the wt and each mutant protein. Lanes 1−6 are wt, R116A, K117A, K178A, R122A, and R223A, respectively. An asterisk marks the position of the full-length protein. The minor bands below the full-length protein band were the result from the small amount of degradation of the full-length protein.

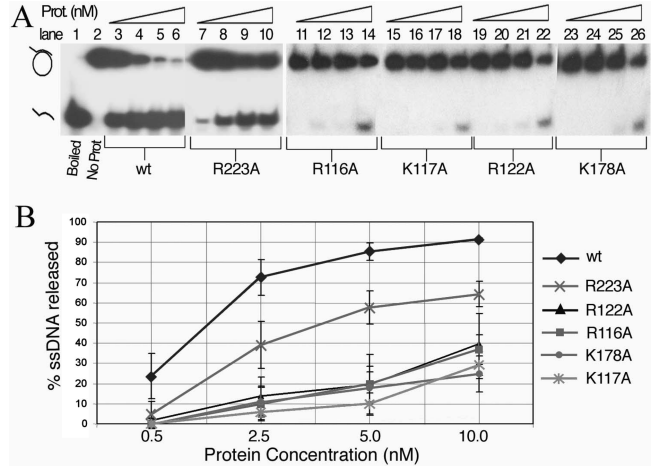

FIGURE 3: Helicase activity of wt and mutant proteins. A: Gel analysis of helicase assay. Increasing concentrations of wt (lanes 3−6), R223A (lanes 7−10), R116A (lanes 11−14), K117A (lanes 15−18), R122A (lanes 19−22), and K178A (lanes 23−26) were incubated with radiolabeled helicase substrate at 50 °C for 30 min, and samples were then analyzed by 12% polyacrylamide gel electrophoresis. Boiled and no protein controls are in lanes 1 and 2, respectively. B: Quantitation of unwinding in panel A, expressed as percentage of ssDNA released from the dsDNA substrate. Protein concentrations were calculated based on double hexamer molecular weights. Error bars (SEM) are from a minimum of three independent experiments.

RESULTS

Location of Mutated Residues on the mtMCM Double-Hexamer Structure. The crystal structure of the N-terminal region of mtMCM (N-mtMCM) shows that the five residues (R116, K117, R122, K178, R223) studied here are located

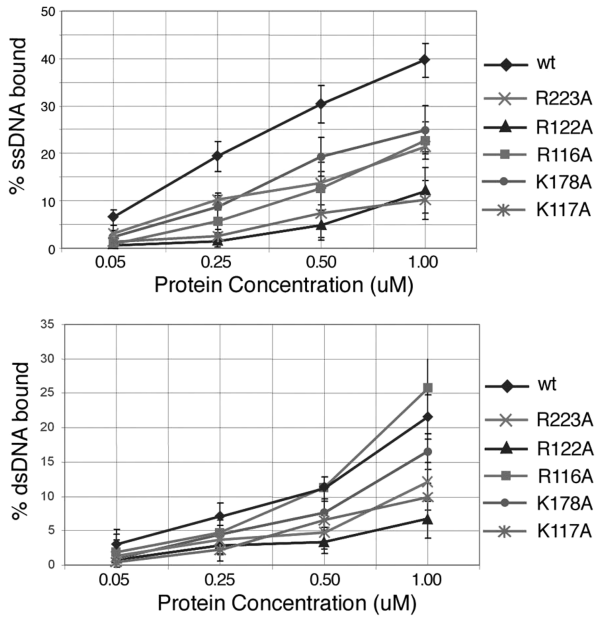

FIGURE 4: DNA binding of wt and mutants. A: Quantitation of ssDNA binding of wt and mutants at the indicated protein concentrations. B: Quantitation of dsDNA binding of wt and mutants at the indicated protein concentrations. Protein concentrations were calculated based on double hexamer molecular weights. Error bars (SEM) are from a minimum of three independent experiments.

close to the central channel surface (Figure 1A,B). K117, R122, and K178 are highly conserved among eukaryotic MCMs (Figure 1C). R223 is not strictly conserved, but there appear to be few positively charged residues in the vicinity of R223 among the aligned MCM sequences and R116 appears to be unique to mtMCM (Figure 1C). R116, K117, and R122 are located on the same β-strand and K178 is on the adjacent antiparallel β-strand (Figure 1A,B). R223 is located on the previously characterized DNA binding β-hairpin finger (*10*) and is close to the cluster of the other mutated amino acids.

Mutant Protein Assembly and Stability. We first performed experiments to test the structural integrity of the mutant mtMCM proteins in order to rule out the possibility of disruption of protein folding or assembly by the mutations. All mutant proteins and the wild-type (wt) protein were analyzed by FPLC using an analytical Superose-6 gel filtration column before and after the proteins were heat-treated at 55 °C. With or without heat treatment, all mutants had similar chromatographic profiles as the wt, characterized by a peak (P2) with an apparent molecular weight of a double hexamer of mtMCM (Figure 2A). SDS−PAGE of fractions collected across this peak revealed a predominant band consistent with the size of the full-length protein (Figure 2B). N-terminal sequencing showed that other minor bands were degradation products of the full-length protein that could not be completely eliminated even after extensive purification. As all mutants and wt showed similar extents of degradation, the degradation should not interfere with the comparison and interpretation of biochemical results. The chromatography analysis indicated that none of the mutations affected mtMCMs folding, oligomerization state, or heat stability in solution.

Helicase Assay. A helicase assay showed that the mutants had various degrees of reduced helicase activity when compared with the wt protein (Figure 3A,B). Over the tested protein concentration range, helicase activity of R223A was 2−4 fold lower than the activity of the wt protein and the helicase activities of R116A, K117A, R122A, and K178A were 3−7 fold lower that that of the wt (Figure 3A,B). This suggests that these charged residues are important for the helicase activity of mtMCM.

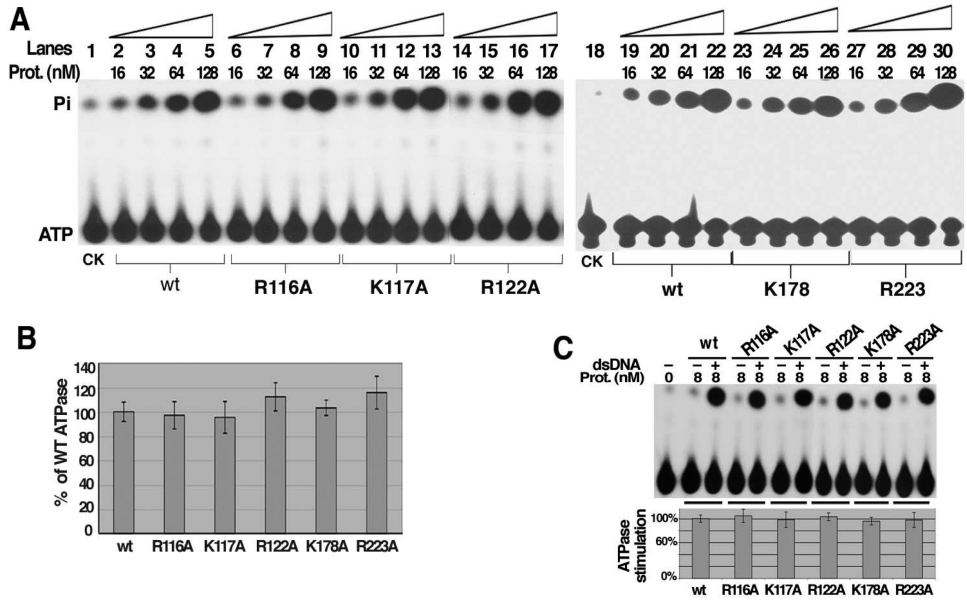

FIGURE 5: ATPase activity of the wt and mutants. A: TLC analysis of ATPase assay. Four protein concentrations, 16, 32, 64, and 128 nM, were used for wt (lanes 2−5 and 19−22), R116A (lanes 6−9), K117A (lanes 10−13), R122A (lanes 14−17), K178A (lanes 23−26), and R223A (lanes 27−28). No protein control is in lanes 1 and 18. B: Quantitation of results from panel A. Protein concentrations were calculated based on double hexamer molecular weights. C: TLC analysis of ATPase assay of the mutants in the presence of dsDNA (10 ng/μL 1.0 kb PCR DNA product), showing that all mutants responded to dsDNA stimulation of ATPase activity similarly to the wt. The chart on the bottom is an quantitation of ATPase stimulation results. Error bars (SEM) in all charts are from a minimum of three independent experiments.

DNA Binding. The ability of wt and mutants to bind single-stranded DNA (ssDNA) and double-stranded DNA (dsDNA) was determined by native gel shift using a radiolabeled oligonucleotide and four different concentrations for each protein. All mutants showed reduced ssDNA binding compared to wt (Figure 4A). At the protein concentration of 1 μM, the ssDNA binding activity for K117A and K178A was approximately 4 fold lower than that for the wt, and for the other three mutants (R116A, R122A, R223A), it was roughly 2 fold lower than wt. dsDNA binding assay results were quite similar to those of the ssDNA binding analysis (Figure 4B). Four out of the five mutants (K117A, R122A, K178A, R223A) showed lower dsDNA binding (approximately 2−4 fold) than the wt (Figure 4B). However, R116A bound to dsDNA at a level similar to the wt protein.

ATPase Activity. The effect of each mutation on the ability of mtMCM to hydrolyze ATP was measured using standard ATPase assays. The mutations (R116A, K117A, R122A, K178A, R223A) had little effect on the level of ATP hydrolysis when compared to wt (Figure 5A−C), suggesting that none of the residues are directly involved in ATP binding or hydrolysis.

DISCUSSION

The charged residues under investigation (R116, K117, R122, K178, and R223) are all located on the inner central channel surface of the N-mtMCM, a location potentially important for interacting with DNA, which binds within the central channel, and for helicase function. We showed here that mutation of any of these five residues to alanine resulted in lower helicase activity compared with the wt protein. Although all mutants showed ATPase activity comparable to that of wt, all five mutants had consistently reduced ssDNA binding and four out of the five mutants showed reduced dsDNA binding, an observation consistent with the role of these residues in interaction with DNA.

Even though the positively charged residues mutated in this study are all located on the inner channel of the double hexamer, the five residues have different degrees of exposure to the channel surface. For example, R122, R116, and K117 are located on the side of the monomer that faces the next monomer within the ring (Figure 1A,B), forming the edge around the wide-open side of the channel. These three residues are not as exposed to the channel surface as R122 and K178. In order to directly contact DNA, a modest conformational change would be required to expose these residues more to the inner channel surface. Alternatively, DNA may interact with these residues by binding or passing the side channel, as suggested in the looping model of SV40 LTag (*14–16*).

Furthermore, the location of the residues near the interface between two adjacent subunits (R122, R116, K117) may influence the interactions between two neighboring monomers during conformational changes necessary for helicase function. Of the residues evaluated, R122 has been shown to have direct contact with the next neighbor through the β-hairpin (Figure 1B). Indeed, of the mutants analyzed, R122A, R116A, and K117A showed the most significant reduction in ssDNA and dsDNA binding (Figure 4) as well as in helicase function (Figure 3). R116, K117, and R122 are conserved among most *S. cerevisiae* and human MCMs (Figure 1C), suggesting the importance of these residues for MCM function.

Based on the N-mtMCM structure, R223 sits on the previously characterized DNA binding β-hairpin structure that has been shown to be important for helicase function (*10, 17*). Previously, double or triple mutations of three other positively charged residues on this β-hairpin, R226, R229, and K231, were shown to completely disrupt the DNA binding and helicase function. Intriguingly, point mutation of R223 to alanine only partially disrupted MCM DNA binding and helicase activity (Figure 3, Figure 4), suggesting that the multiple positively charged residues on the β-hairpin may be partially complementary to each other.

In summary, this mutational study clearly demonstrated that the positively charged residues on the inner central channel, R116, K117, R122, K178 and R223, are critical for the functional activities of mtMCM. Mutation of any of these residues resulted in decreased helicase activity, which was strongly associated with reduced binding to both ssDNA and dsDNA. Even though these residues are located outside of the highly conserved MCM box (helicase domain), the critical residues for classifying MCM proteins, four of the five residues are highly conserved in eukaryotes, underscoring the functional significance of these charged residues of the hexameric channel surface of the N-terminal region of MCM.

SUPPORTING INFORMATION AVAILABLE

Comparison of the wt mtMCM and the double mutant on the full length mtMCM. This material is available free of charge via the Internet at http://pubs.acs.org.

REFERENCES

1. Neuwald, A. F., Aravind, L., Spouge, J. L., and Koonin, E. V. (1999) AAA+: A class of chaperone-like ATPases associated with the assembly, operation, and disassembly of protein complexes. *Genome Res. 9*, 27–43.
2. Tye, B. K. (1999) Minichromosome maintenance as a genetic assay for defects in DNA replication. *Methods 18*, 329–334.
3. Lei, M., and Tye, B. K. (2001) Initiating DNA synthesis: from recruiting to activating the MCM complex. *J. Cell Sci. 114*, 1447–1454.
4. Kelman, Z., and White, M. F. (2005) Archaeal DNA replication and repair. *Curr. Opin. Microbiol. 8*, 669–676. Epub 2005 Oct 20.
5. Tye, B. K. (1999) MCM proteins in DNA replication. *Annu. Rev. Biochem. 68*, 649–686.
6. Bell, S. P., and Dutta, A. (2002) DNA replication in eukaryotic cells. *Annu. Rev. Biochem. 71*, 333–374. Epub 2001 Nov 9.
7. Forsburg, S. L. (2004) Eukaryotic MCM proteins: beyond replication initiation. *Microbiol. Mol. Biol. Rev. 68*, 109–131, table of contents.
8. Shechter, D., Ying, C., and Gautier, J. (2000) The intrinsic DNA helicase activity of M. thermoautotrophicum delta H minichromosome maintenance protein. *J. Biol. Chem. 275*, 15049–15059.
9. Chong, J., Hayashi, M., Simon, M., Xu, R., and Stillman, B. (2000) A double-hexamer archaeal mini-chromosome maintenance protein is an ATP-dependent DNA helicase. *Proc Natl Acad Sci U.S.A. 97*, 1530–1535.
10. Fletcher, R. J., Bishop, B. E., Leon, R. P., Sclafani, R. A., Ogata, C. M., and Chen, X. S. (2003) The structure and function of MCM from archaeal M. Thermoautotrophicum. *Nat. Struct. Biol. 10*, 160–167.
11. Kelman, Z., Lee, J., and Hurwitz, J. (1999) The single minichromosome maintenance protein of M. thermoautotrophicum DeltaH contains DNA helicase activity. *Proc Natl Acad Sci U.S.A. 96*, 14783–14788.

12. Fletcher, R. J., Shen, J., Gomez-Llorente, Y., Martin, C. S., Carazo, J. M., and Chen, X. S. (2005) Double hexamer disruption and biochemical activities of Methanobacterium thermoautotrophicum MCM. *J. Biol. Chem. 280*, 42405–42410. Epub 2005 Oct 11.
13. Kasiviswanathan, R., Shin, J. H., Melamud, E., and Kelman, Z. (2004) Biochemical characterization of the Methanothermobacter thermautotrophicus minichromosome maintenance (MCM) helicase N-terminal domains. *J. Biol. Chem. 279*, 28358–28366. Epub 2004 Apr 20.
14. Li, D., Zhao, R., Lilyestrom, W., Gai, D., Zhang, R., DeCaprio, J. A., Fanning, E., Jochimiak, A., Szakonyi, G., and Chen, X. S. (2003) Structure of the replicative helicase of the oncoprotein SV40 large tumour antigen. *Nature 423*, 512–518.
15. Gai, D., Zhao, R., Li, D., Finkielstein, C., and Chen, X. (2004) Mechanisms of conformational change for a replicative hexameric helicase of SV40 large tumor antigen. *Cell 119*, 47–60.
16. Sclafani, R., Fletcher, R., and Chen, X. (2004) Two heads are better than one: regulation of DNA replication by hexameric helicases. *Genes Dev. 18*, 2039–2045.
17. McGeoch, A. T., Trakselis, M. A., Laskey, R. A., and Bell, S. D. (2005) Organization of the archaeal MCM complex on DNA and implications for the helicase mechanism. *Nat. Struct. Mol. Biol. 14*, 14.

BI800032T